

COMPUTATIONAL ANALYSIS OF STATIC AND DYNAMIC BEHAVIOUR OF MAGNETIC SUSPENSIONS AND MAGNETIC BEARINGS

Dr. Colin P. Britcher
Department of Aerospace Engineering
Old Dominion University
Norfolk, VA 23529-0247

and

Nelson J. Groom
Guidance and Control Branch
Flight Dynamics and Control Division
NASA Langley Research Center
Hampton, VA 23681

ABSTRACT

Static modelling of magnetic bearings is often carried out using magnetic circuit theory. This theory cannot easily include nonlinear effects such as magnetic saturation or the fringing of flux in air-gaps. Modern computational tools are able to accurately model complex magnetic bearing geometries, provided some care is exercised. In magnetic suspension applications, the magnetic fields are highly three-dimensional and require computational tools for the solution of most problems of interest.

The dynamics of a magnetic bearing or magnetic suspension system can be strongly affected by eddy currents. Eddy currents are present whenever a time-varying magnetic flux penetrates a conducting medium. The direction of flow of the eddy current is such as to reduce the rate-of-change of flux. Analytic solutions for eddy currents are available for some simplified geometries, but complex geometries must be solved by computation. It is only in recent years that such computations have been considered truly practical. At NASA Langley Research Center, state-of-the-art finite-element computer codes, "OPERA", "TOSCA" and "ELEKTRA" have recently been installed and applied to the magnetostatic and eddy current problems.

This paper reviews results of theoretical analyses which suggest general forms of mathematical models for eddy currents, together with computational results. A simplified circuit-based eddy current model proposed appears to predict the observed trends in the case of large eddy current circuits in conducting non-magnetic material. A much more difficult case is seen to be that of eddy currents in magnetic material, or in non-magnetic material at higher frequencies, due to the lower skin depths. Even here, the dissipative behaviour has been shown to yield at least somewhat to linear modelling.

Magnetostatic and eddy current computations have been carried out relating to the Annular Suspension and Pointing System, a prototype for a space payload pointing and vibration isolation system, where the magnetic actuator geometry resembles a conventional

magnetic bearing. Magnetostatic computations provide estimates of flux density within air-gaps and the iron core material, fringing at the pole faces and the net force generated. Eddy current computations provide coil inductance, power dissipation and the phase lag in the magnetic field, all as functions of excitation frequency. Here, the dynamics of the magnetic bearings, notably the rise time of forces with changing currents, are found to be very strongly affected by eddy currents, even at quite low frequencies.

Results are also compared to experimental measurements of the performance of a large-gap magnetic suspension system, the Large Angle Magnetic Suspension Test Fixture (LAMSTF). Eddy current effects are again shown to significantly affect the dynamics of the system.

Some consideration is given to the ease and accuracy of computation, specifically relating to OPERA/TOSCA/ELEKTRA.

INTRODUCTION

The prediction of magnetostatic forces in small-gap magnetic suspensions, most notably magnetic bearings, has typically relied heavily on so-called "circuit models" [1,2]. Here, the magnetomotive force and reluctances around the closed flux path are equated to give the total flux in the circuit. Experience has shown that where the air-gap is small and the flux path is properly designed, these calculations are fairly reliable. Some cases arise, however, where extra precision is required, or where the variation of flux across the air-gap is of interest [3]. In large-gap magnetic suspension systems, no simple predictive model exists, due to the highly three-dimensional flux path [4,5]. Hence there is an increasing use of finite element, magnetostatic computer codes for design and analysis of both small-gap and large-gap systems.

Where the dynamics of magnetic actuators are of interest, it has been shown that eddy currents in conducting cores, metallic structures, etc., can cause significant departures from ideal behaviour [6,7]. Potentially the most troubling are restrictions on the bandwidth of such actuators. Here, the problem is sufficiently complex such that some form of finite element approach is recommended throughout.

APPLIED COMPUTATIONAL ELECTROMAGNETICS

Finite element methods are used extensively to obtain solutions to a wide range of engineering problems governed by partial differential, or integral equations. Numerical solutions become possible for problems with complex geometries, awkward boundary conditions and/or nonlinear behaviour. It is not the purpose of this paper to describe the difficulties of the approach, the formulations or numerical methods used in any detail, since a vast quantity of literature exists [8,9,10 etc.]. Rather, an existing "state-of-the-art" suite of codes is applied to real-world problems related to magnetic bearings and magnetic suspensions. The apparent accuracy of the solutions, with comparison to experimental data where possible, the practical problems encountered, and the weaknesses revealed in the codes, are all addressed from an applications perspective.

Magnetostatic fields can be expressed as a sum of a solenoidal component (where no current is flowing) and a rotational component (inside current-carrying conductors). In the solenoidal region, simple potential functions should describe the magnetic field, although a

difficulty arises exterior to current-carrying conductors, where the potential is multi-valued. This difficulty can be overcome by splitting the field into two parts, one representing the field due to magnetized volumes, and another representing the contribution of current-carrying conductors. A "reduced potential" can be defined to represent the former, and a "total potential" to represent the combination. The total potential can now be made single-valued in regions exterior to current-carrying conductors. The field due to prescribed currents (i.e. prescribed currents in electromagnet windings) is calculated in the reduced potential space using the Biot-Savart law. For practical eddy current problems, the governing equations are the zero-frequency limit of Maxwell's equations. This implies that the wavelength of any electromagnetic wave is very long compared to the characteristic physical dimension of the problem. These equations can be solved using a "vector potential" formulation, where $B = \nabla \times A$. The region containing an eddy current problem can therefore be subdivided into reduced, total and vector potential spaces as appropriate, with field continuity enforced on the boundaries between different potentials. The approach described is the one used in this work, but is far from being the only possibility.

OPERA-3D / TOSCA / ELEKTRA / VF-GFUN

OPERA-3D (OPerating environment for Electromagnetic Research and Analysis) comprises an interactive, graphical, pre-processor, for preparation of finite element problems, with a related post-processor, for analysis and display of results. Problems specified in the pre-processor are submitted to a variety of analysis packages for solution. These packages include TOSCA, for solution of magnetostatic and electrostatic problems using conventional finite-element methods, VF/GFUN, for solution of magnetostatic problems using integral equation methods, and ELEKTRA, for solution of eddy current problems using the finite-element method.

THE ANNULAR SUSPENSION AND POINTING SYSTEM

The Annular Suspension and Pointing System (ASPS) is a prototype for a high precision space payload pointing and vibration isolation system. A ferromagnetic rotor is magnetically suspended by five double-acting magnetic bearing stations, such that the orientation of the ring can be controlled in two "tilt" and three translational degrees-of-freedom, with a high level of isolation of base vibrations. The general configuration is illustrated in Figure 1, with the geometry of one of the "axial" bearing stations shown in Figure 2. Considerable hardware upgrades have been made recently, and the system now utilizes transistor switching power amplifiers and a simple digital controller [11]. Further details are presented elsewhere in this Proceedings [12].

THE LARGE-ANGLE MAGNETIC SUSPENSION TEST FIXTURE (LAMSTF)

In order to explore the technology required for the magnetic suspension of objects over large ranges of orientation, a small-scale laboratory development system, the Large Angle Magnetic Suspension Test Fixture (LAMSTF) was constructed at NASA Langley Research

Center. Possible applications for magnetic suspension systems of this general class include space payload pointing and manipulation, microgravity vibration isolation and wind tunnel model suspension. An important objective of this particular project is to investigate the dynamic modelling of large-gap magnetic suspension systems, so that future systems can be designed with higher levels of confidence.

The general configuration [13] is illustrated in Figure 3. Five room temperature copper electromagnets are mounted on an aluminum plate, each electromagnet driven by a transistor switching power amplifier. The suspended element consists of Neodymium-Iron-Boron permanent magnet material inside an aluminum tube. The direction of magnetization is along the axis of the cylinder, which is horizontal when suspended. The suspension height is 0.1m, measured from the axis of the suspended element to the top plane of the electromagnet conductor. Several different control systems have been developed and demonstrated, including several digital versions [14, 15].

MAGNETOSTATIC CALCULATIONS - SMALL AIR-GAPS

A simplified finite element representation of an ASPS axial bearing station is shown in Figure 4. Only one "side" of the real actuator is represented, corresponding to the present operational status where the rotor is suspended against gravity. It should also be noted that the rotor cross-section is considerably simplified, with the cylindrical inner flange and rotor curvature deleted. This permits more extensive symmetry in the problem and a reduction in solution time. A linear TOSCA solution for a current of 1 Amp in both coils and an iron relative permeability of 1000 is also seen in Figure 4.

A comparison of the predicted magnetic fluxes in the center of the air-gap is shown in Table A. The air-gap is 3.41 mm and the coil current 1 A for these cases. The discrepancy between the circuit model and both computational or experimental results is quite large and worrisome. The major problem is quickly found to be the improper assumption (in the circuit model) of uniform magnetic flux in the air-gap. The air-gap in ASPS is relatively large by the standards usually applied to magnetic bearings, the "aspect ratio" (diameter/gap) being between 6 (original design) and 12 (modified axial stations). Flux "fringing" around the periphery of the air-gap is, therefore, quite pronounced, as indicated in Figure 5.

TABLE A - Flux at gap centroid

TOSCA solution, $\mu=1000$, Tesla	0.2385
Measured, Ni-Fe core, Tesla	0.2010
Circuit model, $\mu \rightarrow \infty$, Tesla	0.2985

It has previously been suggested that the predicted and actual magnetic forces would be in closer agreement, since the circuit model overpredicts gap flux, but confines the flux to an underpredicted area. The comparison between predicted, computed and measured forces does indicate improved agreement, but still significant discrepancies, as shown in Table B. The total flux crossing the air-gap is also compared between the circuit model and computations.

Studies were undertaken during the original development of ASPS to improve the accuracy of the circuit model by accounting for fringing and leakage path reluctances. Due to the difficulties and limited scope of this approach, the circuit model is now abandoned as a

viable, accurate tool in this case. Instead, further refinement of the finite element solution will be addressed.

TABLE B - Flux and forces per air-gap

	Total flux, Tm ²	Force, N
TOSCA, $\mu=1000$	5.87e-4	44.47
Circuit model, $\mu \rightarrow \infty$	4.9e-4	58.2
Experimental, assuming rotor mass	<i>not available</i>	41.79

Once a basic finite element model has been established, the usual and proper procedure to establish a satisfactory confidence level in the results is to study the effects of variations of detail parameters within the model. The classic example is grid refinement, where a nearly stationary result with increasing refinement indicates that the grid is "sufficiently" fine. Here, this idea can be extended to introducing quadratic elements in critical regions, such as in and around the air-gap, and local refinement of the grid in regions of high field gradients. Further, a realistic BH curve can be invoked, the resulting solution being magnetically nonlinear. Typical results from these studies are shown in Table C. It is emphasized that the initial results from any finite element solution should be regarded with some scepticism. Studies of solution accuracy and realism are always a sensible investment of time and effort.

From a reliable solution, valuable qualitative design information is easily obtained, as illustrated in Figure 6. Here it is seen that the highest flux density in the magnetic circuit occurs at an interior corner of the flux return path. This corner should clearly be radiused to improve the linearity of the assembly close to overall saturation.

It should be noted that TOSCA is capable of solving problems with anisotropic materials. This capability is not, however, demonstrated here, since the ASPS core material is not laminated and is thought to be quite isotropic.

TABLE C - Flux at gap centroid

8008 linear elements, $\mu=1000$	0.2385
8008 quadratic elements, $\mu=1000$	0.2392
16,170 linear elements, $\mu=1000$	0.23875
8008 linear elements, μ =mild steel	0.20587
8008 linear elements, μ =high grade steel	0.22677

MAGNETODYNAMIC CALCULATIONS - SMALL AIR-GAPS

A finite element model similar to that described above can be submitted to the ELEKTRA solver, for analysis of eddy currents induced in the iron cores by sinusoidal currents in the electromagnets. Magnetically nonlinear or anisotropic problems are not presently soluble with ELEKTRA. Some care proved to be necessary to establish an effective combination of total, reduced and vector potentials. In this case, it was found to be necessary to "coat" the surface of the iron region with a layer of vector potential air, in order to improve the solution matrix conditioning in the presence of abrupt changes in magnetic and electrical properties at the iron-air interface. Establishing a valid configuration, favorable element

distributions, and the correct boundary conditions are practical problems that do require some familiarity with whichever codes are used, and a certain degree of skill and experience.

An effort to model, measure and compute the eddy current effects in the ASPS bearing stations has begun. Magnetic field in the air-gap is measured using a Hall-effect gaussmeter with the rotor locked in its datum position. Early experimental results indicate steadily falling magnetic field intensity in the air-gap and steadily increasing phase lag, as frequency is increased, as shown in Figure 7. The rate of roll-off is seen to be around 10 db/decade as suggested by application of classical theories [8,16,17,18]. There is also a strong indication of variations in relative amplitude and phase of the magnetic field across the air-gap, also shown in Figure 7. A typical eddy current distribution in the iron core is shown in Figure 8.

It should be noted that these computations require the specification of two material properties, namely magnetic permeability and electrical conductivity. Neither is easy to specify accurately for the nickel-iron alloy employed, partly due to the effect of heat-treatments. Since the observed break frequencies depend on the square-root of the product of these two parameters, this is seen to represent a significant practical problem.

Both computational and experimental results indicate an ASPS actuator bandwidth of perhaps 30 Hz. This happens to be well above the design system bandwidth of around 1 Hz, so is not a serious performance limitation. The low design value is due to the massive payloads envisioned (at least 600 kg for the original specifications, later increased).

MAGNETOSTATIC CALCULATIONS - LARGE AIR-GAPS

One of the earliest applications of the OPERA-3D suite of codes in this research was the computation of magnetic fields and field gradients in air, to permit the prediction of forces and moments on the suspended element in LAMSTF. Where the suspension coils are air-cored and the suspended element is a permanent magnet, no finite element solution is required. Instead, the field in air due to prescribed currents can be calculated directly by numerical integration of the Biot Savart law (by OPERA), to very high accuracy. When iron cores are present in the suspension coils, the magnetization must be determined as part of the solution. Extensive use has been made of VF/GFUN in this application. The integral equation approach used in VF/GFUN only requires the discretization of the iron regions and thus seems to be a more appropriate approach for this class of problem.

Computed fields have been compared to experimental measurements in a variety of cases. Typical agreement, such as shown in Figure 9, has been considered satisfactory, especially considering the considerable problems inherent in accurate experimental measurements of highly 3-dimensional fields. In fact, computations have often been regarded as more consistently reliable, particularly in estimating field gradients. Forces and moments on the suspended object can be calculated to good accuracy by integration of the Maxwell stress tensor on a control surface surrounding the object [5,9 etc.].

MAGNETODYNAMIC CALCULATIONS - LARGE AIR-GAPS

In the original design of LAMSTF, eddy-current circuits were deliberately introduced in three main areas: the position sensor structure, the electromagnet cores, and the aluminum baseplate. This was done so that it would be necessary to measure, analyze and model the eddy

current effects, rather than attempting to avoid their influence, as would have been the conventional practice. The fact that stable suspension was initially achieved rather easily was taken to indicate that the eddy current effects were not very significant. However, a consistent discrepancy was discovered in the dynamic behaviour in the "pitch" degree-of-freedom [7,13], when the metallic baseplate and sensor frame were used. This led to a careful analysis of the effects of eddy currents, which were subsequently confirmed to be the cause of the anomaly.

A typical result, relating to the eddy currents flowing in the position sensor ring is shown in Figure 10. Further results have been more fully described elsewhere [7,17]. Good agreement between experiment and computation is observed for simple geometries, but significant difficulties are encountered with more complex geometries.

DISCUSSION

No finite element code of this level of sophistication can be considered particularly easy to use by the novice. Potential users interested more in applications engineering than the codes themselves should exercise extreme care in interpretation of results and should be prepared to invest in training of some kind and experimental validation where possible. Further, the suite of codes employed here do lack certain desirable features. These include the ability to model hysteresis and the ability to model anisotropic materials or rotational motion in magnetodynamic problems. Other commercially available codes have comparable weaknesses, although developments are proceeding at a rapid pace. It should be noted that currently available codes represent truly astounding advances in capability from anything available even a decade ago.

CONCLUSIONS

Contemporary software provides powerful tools for the analysis of magnetic fields, forces and moments, and eddy currents in magnetic suspensions and magnetic bearings. Results compare reasonably well to experimental measurements, provided care is exercised and accurate material properties are available.

ACKNOWLEDGEMENTS

This work was supported by NASA Langley Research Center under Grant NAG-1-1056. The Technical Monitor was Nelson J. Groom of the Guidance and Control Branch, Flight Dynamics and Control Division. The first author would also like to express gratitude to a number of graduate students who have contributed to this work, notably Mehran Ghofrani, Lucas Foster, Daniel Neff and Yan Yang.

REFERENCES

1. Schweitzer, G.; Bleuler, H.; Traxler, A.: Active Magnetic Bearings. vdf Hochschulverlag

AG, 1994

2. Moon, F.C.: Superconducting Levitation. Wiley, 1994
3. Knight, J.D.; Xia, Z.; McCaul, E.B.: Forces in Magnetic Journal Bearings: Nonlinear Computation and Experimental Measurement. 3rd International Symposium on Magnetic Bearings, Alexandria, VA, July 29-31, 1992.
4. Groom, N.J.; Britcher, C.P.: Open-Loop Characteristics of Magnetic Suspension Systems Using Electromagnets Mounted in Planar Arrays. NASA TP-3229, November 1992.
5. Britcher, C.P.: Large-gap Magnetic Suspension Systems. International Symposium on Magnetic Suspension Technology, August 1991, published as NASA CP-3152, 1992.
6. Kim, C.; Palazzolo, A.B.; Tang, P.; Manchala, D.; Kascak, A.; Brown, G.; Montague, G.; Klusman, S.: Field Lag Effects on the Vibrations of Active Magnetic Bearing Levitated Rotors. 4th International Symposium on Magnetic Bearings, Zurich, Switzerland, August 23-26, 1994.
7. Britcher, C.P.; Foster, L.: Some Further Developments in the Dynamic Modelling of the Large-Angle Magnetic Suspension Test Fixture. 2nd Int. Symposium on Magnetic Suspension Technology, Seattle, WA, Aug.1993. NASA CP-3247, May 1994.
8. Binns, K.J.; Lawrenson, P.J.; Trowbridge, C.W.: The Analysis and Computation of Electric and Magnetic Fields. Wiley, 1992.
9. Ida, N.; Bastos, J.P.A.: Electromagnetics and Calculation of Fields. Springer Verlag, 1992.
10. Allaire, P.E.; Rockwell, R.; Kasarda, M.E.F.: Magnetic and Electric Field Equations for Magnetic Bearing Applications. MAG'95, Alexandria, VA, August 10-11, 1995.
11. Britcher, C.P.; Groom, N.J.: Current and Future Development of the Annular Suspension and Pointing System, 4th International Symposium on Magnetic Bearings, ETH, Zurich, August 1994.
12. Neff, D.J.; Britcher, C.P.: Design and Implementation of a Digital Controller for a Vibration Isolation and Vernier Pointing System. 3rd International Symposium on Magnetic Suspension Technology, Tallahassee, FL, December 1995.
13. Britcher, C.P.; Ghofrani, M.: A Magnetic Suspension System with a Large Angular Range. Review of Scientific Instruments, Volume 64, No. 7, July 1993.
14. Cox, D.E.; Groom, N.J.: Implementation of a Decoupled Controller for a Magnetic Suspension System using Electromagnets Mounted in a Planar Array. 2nd International Symposium on Magnetic Suspension Technology, Seattle, WA, Aug.1993. NASA CP-3247, May 1994.
15. Lim, K.; Cox, D.E.: Robust Tracking Control of a Magnetically Suspended Rigid Body. 2nd International Symposium on Magnetic Suspension Technology, Seattle, WA, Aug.1993. NASA CP-3247, May 1994.
16. Zmood, R.B.; Anand, D.K.; Kirk, J.A.: The Influence of Eddy Currents on Magnetic Actuator Performance. IEEE Proceedings, Vol.75, No.2, February 1987.
17. Britcher, C.P.; Groom, N.J.: Eddy Current Computations Applied to Magnetic Suspensions and Magnetic Bearings. MAG'95, Alexandria, VA, August 1995.
18. Stoll, R.L.: The Analysis of Eddy Currents. Clarendon, 1974

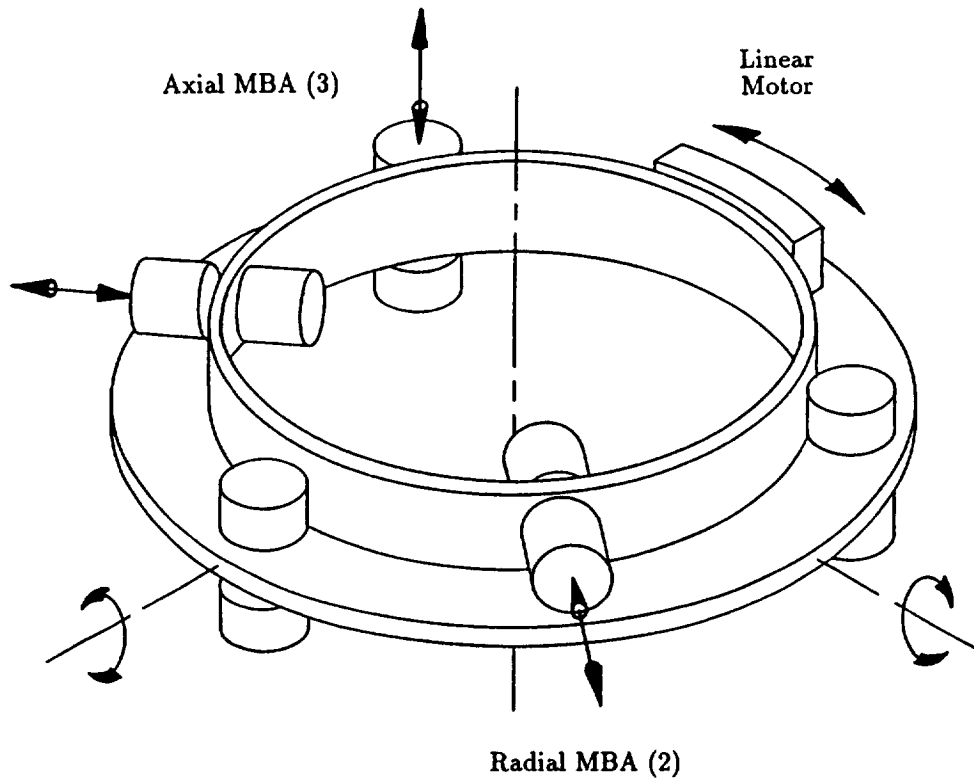


Figure 1 - Geometry of the Annular Suspension and Pointing System

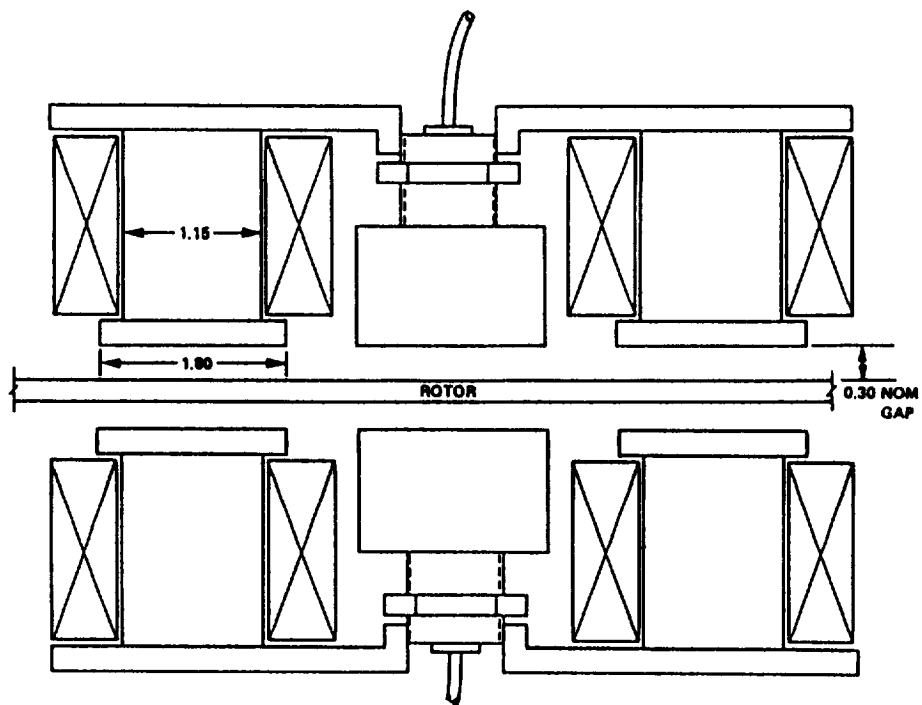


Figure 2 - ASPS Axial Bearing Station (dimensions in inches)

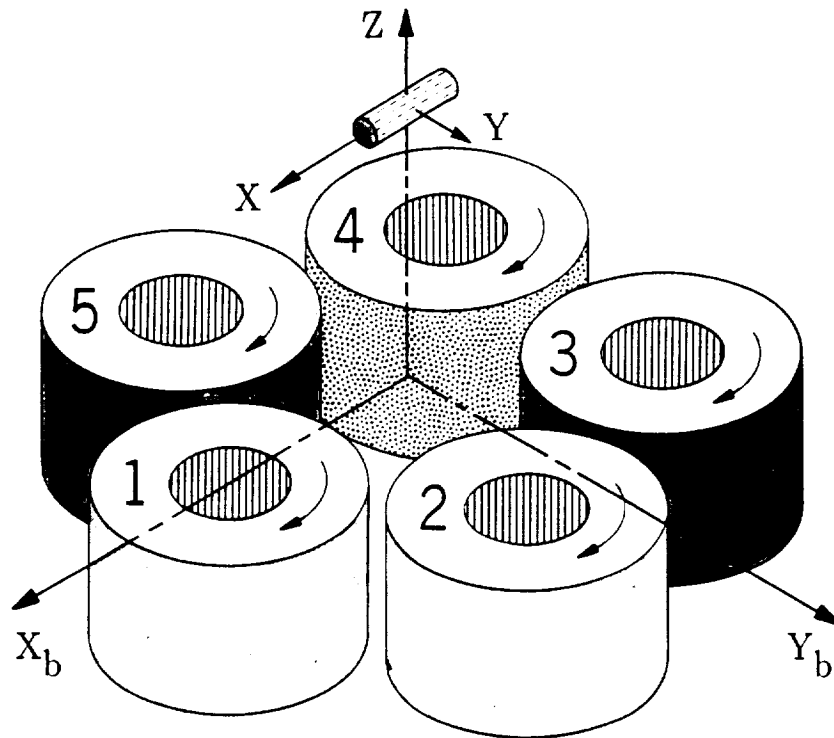


Figure 3 - General Arrangement of the Large Angle Magnetic Suspension Test Fixture

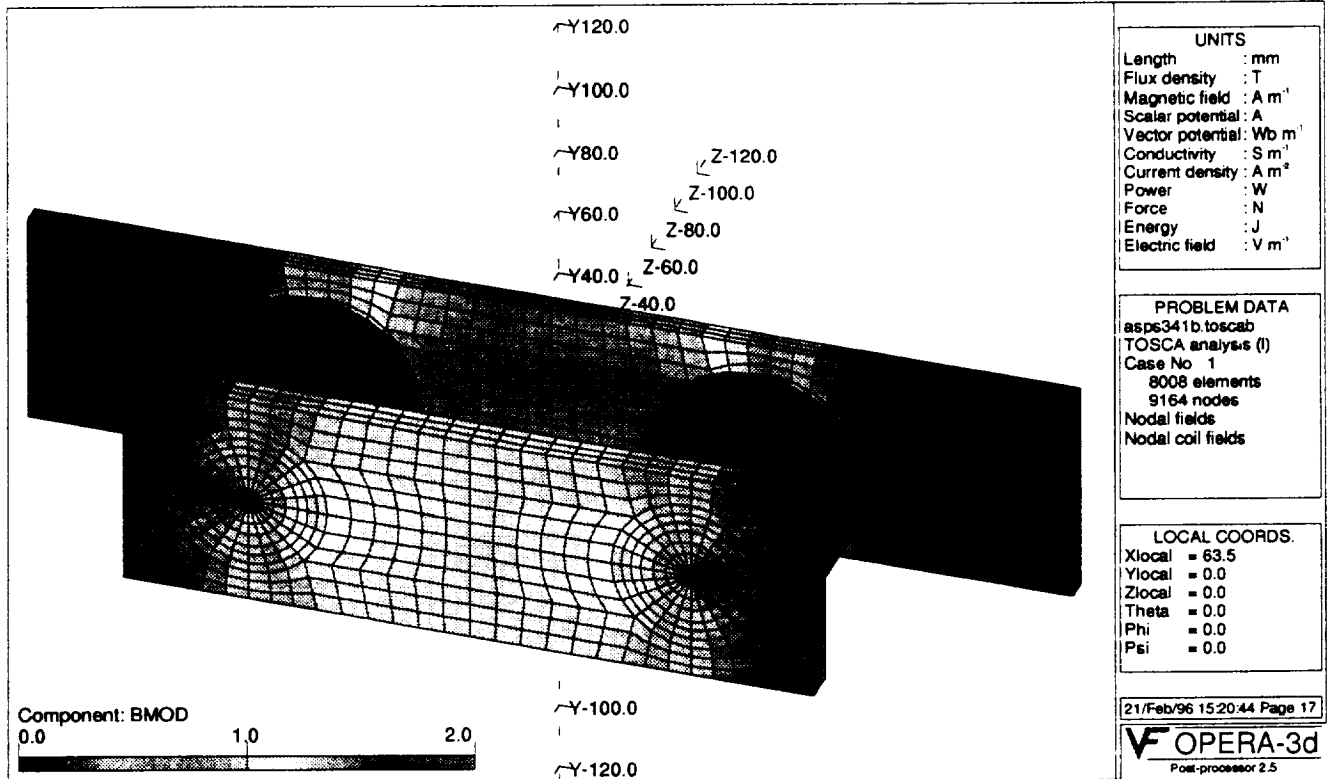


Figure 4 - ASPS Finite Element Model, with TOSCA Solution, $\mu_r=1000$

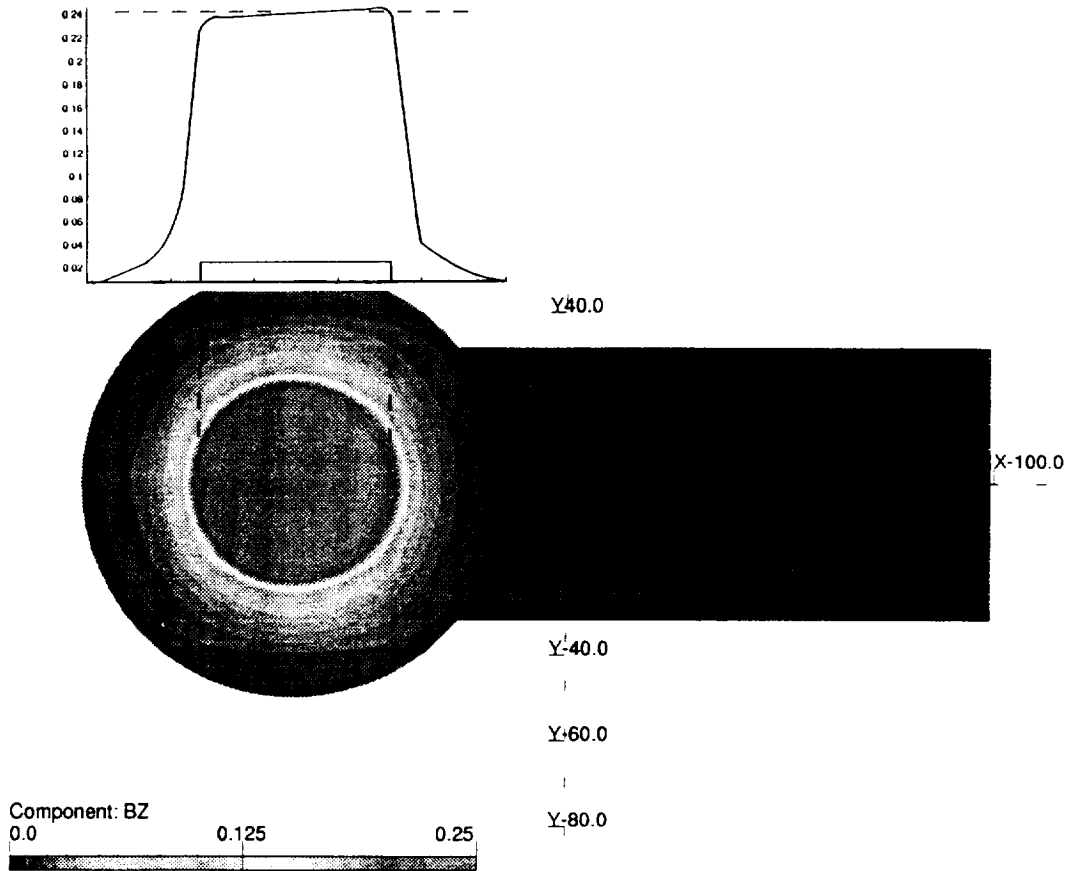


Figure 5 - Computed Magnetostatic Field in Air-Gap, showing flux fringing

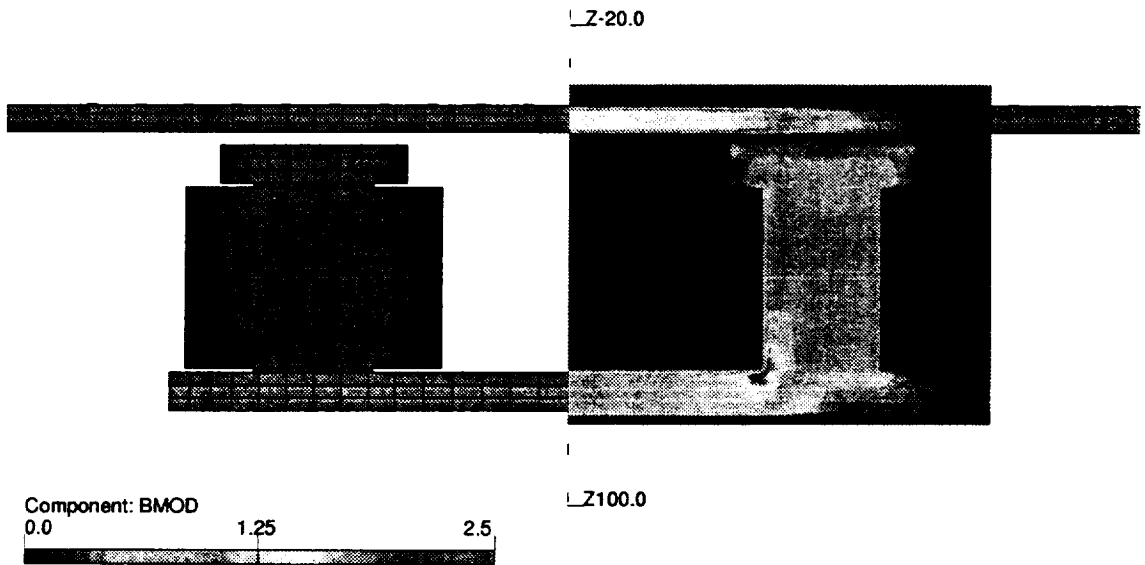
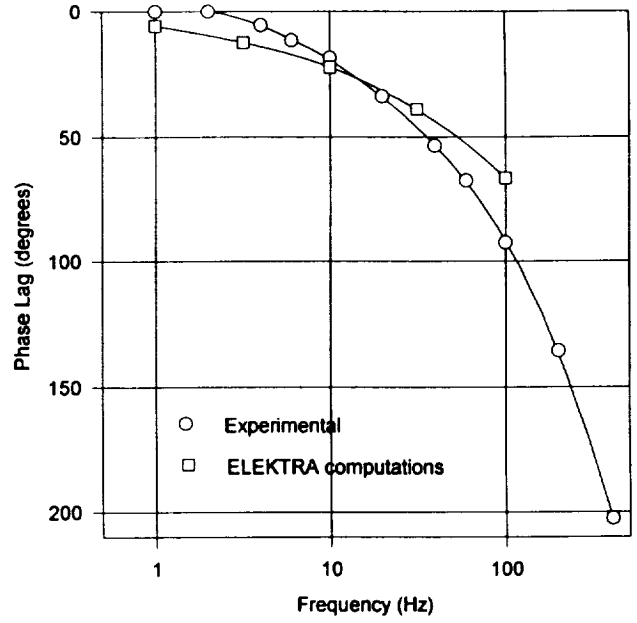
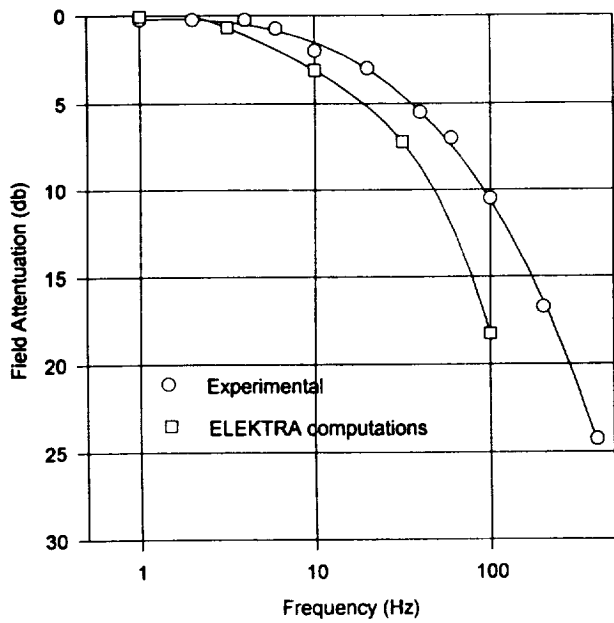
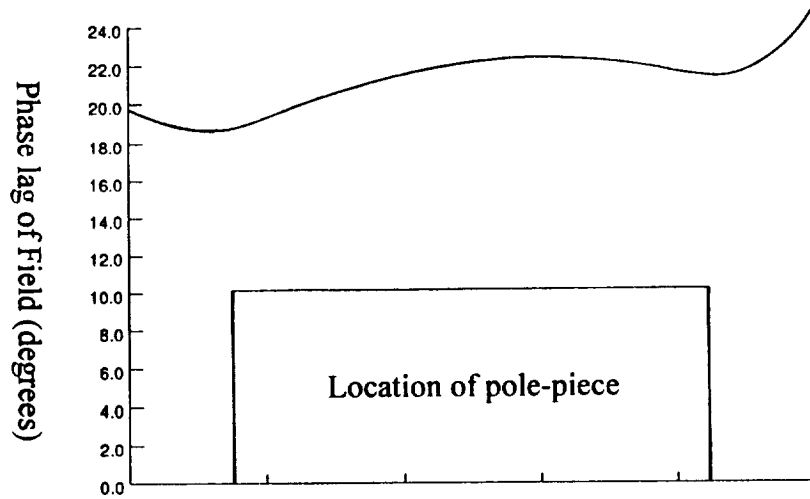


Figure 6 - Magnetic Flux in ASPS Iron Circuit



a) Measured and computed fields at gap centroid



b) Computed phase variation across gap

Figure 7 - Magnetic Fields in the Air-Gap of an ASPS Bearing Station

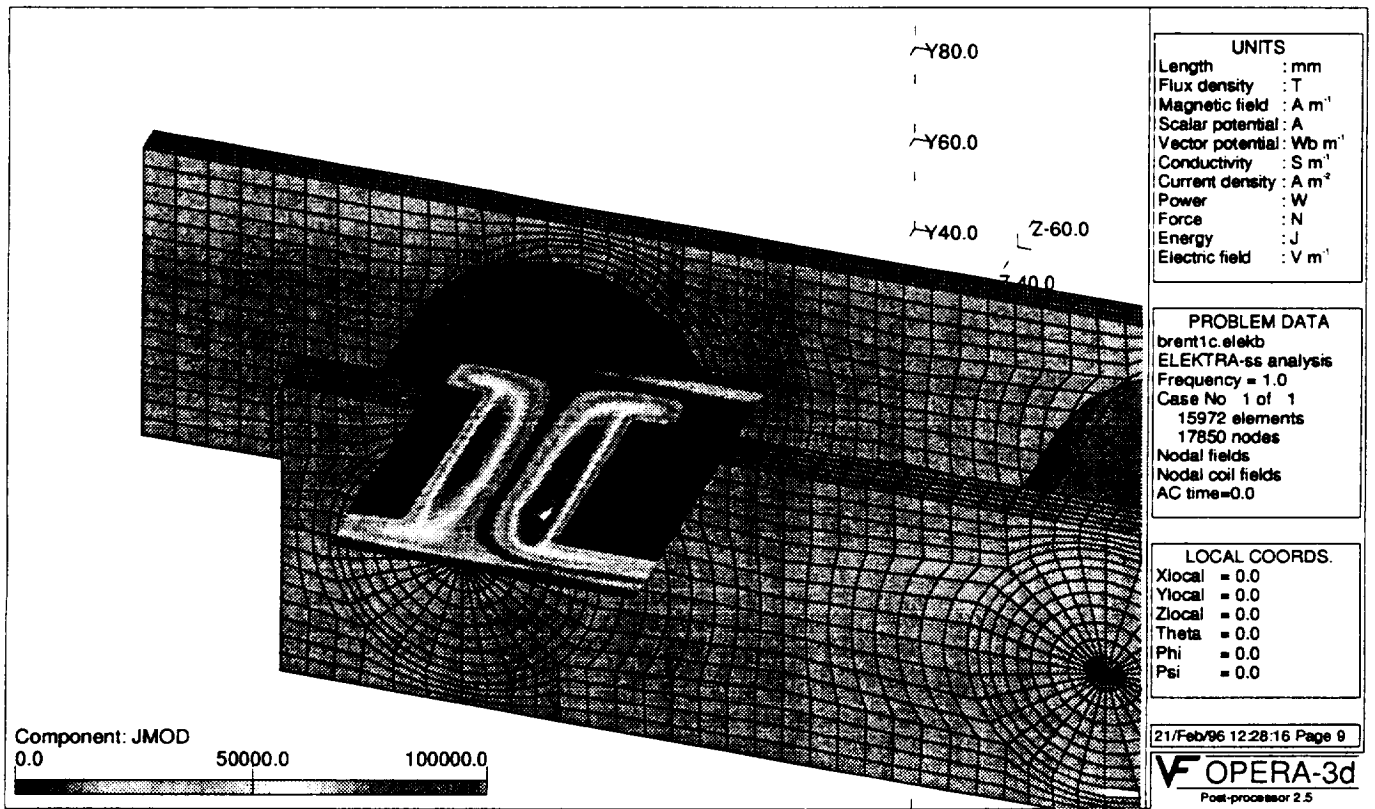


Figure 8 - Eddy Current in ASPS Iron Core

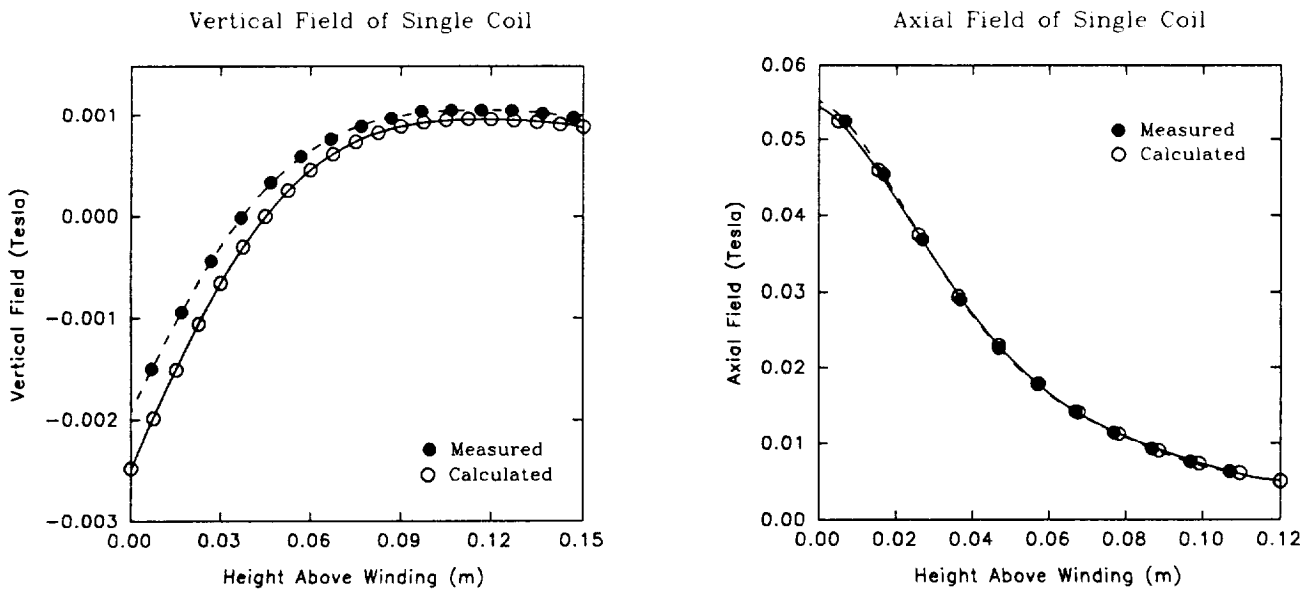


Figure 9 - Typical Air Fields from VF/GFUN

